Fourier transform emission spectroscopy of the $A\ ^2\Pi - X^2\Sigma^+$ system of BeH

C. Focsa,[a] S. Firth,[b] P. F. Bernath,[c] and R. Colin
Laboratoire de Chimie Physique Moléculaire, Université Libre de Bruxelles, C.P. 160/09, 50 av. F. D. Roosevelt, 1050-Brussels, Belgium

(Received 21 May 1998; accepted 2 July 1998)

The $A\ ^2\Pi - X\ ^2\Sigma^+$ transition of BeH was observed by Fourier transform emission spectroscopy using a hollow cathode discharge lamp. The 0–0 to 6–6 bands were rotationally analyzed and molecular constants extracted. The equilibrium rotational constants B_e and bond lengths were found to be 10.331 21(50) cm^{-1} and 1.341 68(3) Å for the ground state and 10.466 31(27) cm^{-1} and 1.332 99(2) Å in the excited state. In order to link the diagonal bands together and to determine the vibrational constants, the 0–1 to 6–7 bands in an archival arc emission spectrum were also rotationally analyzed. In the $X\ ^2\Sigma^+$ and $A\ ^2\Pi$ states, the spectroscopic constants are nearly identical so the $\Delta v = -1$ bands were too weak to be seen in our Fourier transform spectra. Franck–Condon factors were calculated for the $A\ ^2\Pi - X\ ^2\Sigma^+$ transition from Rydberg–Klein–Rees potential curves. These new rotational analyses now link up with the previous work on the 0–7, 0–8, 0–9, 1–9 and 1–10 bands of the $C\ ^2\Sigma^+ - X\ ^2\Sigma^+$ system [R. Colin, C. Drèze, and M. Steinhauer, Can. J. Phys. **61**, 641 (1983)]. Spectroscopic data are thus available for all bound ground state vibrational levels, $v'' = 0-10$, and a set of Dunham Y constants were determined. BeH joins the small group of chemically bound molecules for which a nearly complete set of ground state rovibronic energy levels are known experimentally. © *1998 American Institute of Physics.* [S0021-9606(98)00238-4]

I. INTRODUCTION

The light BeH molecule has been extensively studied by *ab initio* quantum chemists and serves as a test case for open-shell systems (e.g., Refs. 1–9). Partly because of the toxicity of the Be-containing molecules, BeH has been less popular with experimentalists. Watson[10] and Olsson[11] carried out early work on the electronic emission spectra of BeH in the late 1920s and early 1930s. BeH was made by running an arc discharge with Be electrodes in an atmosphere of hydrogen. This early work provided extensive spectra of the $A\ ^2\Pi - X\ ^2\Sigma^+$ system and some data for the $B\ ^2\Pi - X\ ^2\Sigma^+$ system, but of only moderate quality.[10–13] Koontz[14] recorded the $A\ ^2\Pi - X\ ^2\Sigma^+$ transition of BeD and this system has been detected recently in emission from the plasma confined in a tokamak.[15]

The work of Colin and co-workers[16–21] has improved and expanded our spectroscopic knowledge of BeH and BeD and they were even able to study BeT. Improved spectra were recorded by using a carbon tube furnace (King furnace) instead of an arc, and by measuring the bands in absorption. In this way visible, UV, and vacuum UV (VUV) (down to 1700 Å) spectra of BeH and BeD were recorded with the 10 m spectrograph at the National Research Council in Ottawa.[16] These photographic plates allowed a reanalysis of the $A\ ^2\Pi - X\ ^2\Sigma^+$ system and for the assignment of the VUV systems.[19] For reasons of safety the $A\ ^2\Pi - X\ ^2\Sigma^+$ transition of BeT was recorded in a hollow cathode lamp with a 2 m spectrograph.[18] Most recently, the $3d$ Rydberg complex of BeH (and BeD) was analyzed.[21]

All of the known band systems of BeH, BeD, and BeT are very diagonal except for the weak $C\ ^2\Sigma^+ - X\ ^2\Sigma^+$ system that can only be seen in emission from an arc discharge.[20] In addition to the 0–0 to 5–5 bands of the $A\ ^2\Pi - X\ ^2\Sigma^+$ system, the arc produced the 0–7, 0–8, 0–9, 1–9, 2–9, and 1–10 bands of the $C\ ^2\Sigma^+ - X\ ^2\Sigma^+$ system.[20] The tentative identification of the 0–6 band in this work proved to be incorrect. The $C\ ^2\Sigma^+$ state correlates to the same Be $(^3P) + H(^2S)$ asymptote as the $A\ ^2\Pi$ state but has a $r_e = 2.301$ Å compared to $r_e = 1.333$ Å for the $A\ ^2\Pi$ state and $r_e = 1.342$ Å for the $X\ ^2\Sigma^+$ state (see Fig. 1 of Ref. 20). The problem is that the very weak off-diagonal bands of the $A\ ^2\Pi - X\ ^2\Sigma^+$ system only partly link the v' and $v'' = 0-5$ vibrational levels together and there is no direct connection between the $C\ ^2\Sigma^+ - X\ ^2\Sigma^+$ bands and any of the other known ground state vibrational levels ($v'' = 0-5$) in BeH. Fortunately, the $A\ ^2\Pi$ and the $C\ ^2\Sigma^+$ states perturb each other[20] so that an indirect connection could be made and the $v'' = 7-10$ levels of the $X\ ^2\Sigma^+$ state could be located relative to $v'' = 0$.

The dissociation energy ($D_e = 17\,426 \pm 100\ cm^{-1}$) is known for the $X\ ^2\Sigma^+$ state from the limiting curve of

[a]Permanent address: Laboratoire de Physique des Lasers, Atomes et Molécules, UMR CNRS, Centre d'Etudes et de Recherches Lasers et Applications, Université des Sciences et Technologies de Lille, 59 655 Villeneuve d'Ascq Cedex, France.
[b]Present address: Department of Chemistry, University College London, 20 Gordon St., London WC1H0A6, United Kingdom.
[c]Author to whom correspondence should be addressed. Permanent address: Department of Chemistry, University of Waterloo, Waterloo, Ontario N2L 3G1, Canada.

predissociation[20] and from predissociation in the $B\ ^2\Pi$ state.[19] The $v''=10$ level turns out to be the last bound vibrational level of the $X\ ^2\Sigma^+$ state, although $v''=11$ may be bound by a few cm^{-1}. BeH is thus a rather unique system that has spectroscopic data for low vibrational levels ($v''=0-5$, not all linked) and high vibrational levels ($v''=7-10$). If these ground state levels could all be directly linked together and the $v''=6$ gap filled, then the experimental data for BeH would be much more useful. With only five electrons BeH is already widely used to benchmark open-shell *ab initio* methods and to study the breakdown of the Born–Oppenheimer approximation.[8,18]

We report here new Fourier transform emission spectra of the $A\ ^2\Pi-X\ ^2\Sigma^+$ transition for the 0–0 to 6–6 vibrational bands. An attempt was made to link these bands together by observing the vibration–rotation bands as well as the $\Delta v=-1$ bands of the $A-X$ system by Fourier transform emission spectroscopy, but without success. Our hollow cathode source was too weak to see the $\Delta v=-1$ bands and strong thermal emission from the cathode swamped the infrared vibration–rotation emission bands. (There is, however, an infrared spectrum of BeH isolated in an argon matrix.[22]) We, therefore, used unpublished data from the same arc spectrum used for the $C\ ^2\Sigma^+-X\ ^2\Sigma^+$ analysis[20] and identified the 0–1 to 6–7 bands of the $A\ ^2\Pi-X\ ^2\Sigma^+$ system. Thus the $v''=0-10$ levels in the $X\ ^2\Sigma^+$ state and $v'=0-6$ in the $A\ ^2\Pi$ state are now linked together on the same energy scale. BeH thus joins the very small and exclusive group of chemically bound molecules (that includes H_2) for which all of the bound ground state levels are known experimentally.

II. EXPERIMENTAL DETAILS

The $A\ ^2\Pi-X\ ^2\Sigma^+$ $\Delta v=0$ sequence of BeH was excited in a Be hollow cathode discharge and recorded using a Fourier transform spectrometer. Spectra from two different types of hollow cathode discharge lamps were recorded. In the first experiment, we used a water-cooled Be cathode held inside a brass collar and a tungsten ring anode. The cooling water was either off or flowing very slowly. The cathode was operated at currents of ~1.2 A (the maximum that we could get without arcing) and with total pressures of a few Torr with a mixture of 1% H_2 in Ne. Be does not sputter well and the cathode must be very hot to evaporate sufficient metal to make BeH. The Doppler width for well-resolved BeH lines in this relatively cool spectrum was typically 0.15 cm^{-1}, corresponding to a temperature of about 1200 K.

In the second experiment, we recorded a hotter spectrum by using a classical, uncooled Be hollow cathode discharge lamp and with He as the buffer gas. This cathode was not bored through and a tungsten pin anode was used. In this case, the current was ~0.7 A and the total pressure was ~8 Torr with 20% H_2 and 80% He in the nonflowing gas mixture. The BeH rotational lines observed on this second spectrum had measured linewidths of ~0.19 cm^{-1} corresponding to a temperature of about 1500 K. Our best spectrum was recorded just before the cathode melted. The combined study of the two spectra proved to be very useful: while the cooler spectrum provided better resolved lines, the hotter one allowed us to extend the assignment of the branches to higher N values.

The emission from the discharge was recorded with a Bruker IFS 120 HR Fourier transform spectrometer. A Si photodiode detector was used and a bandpass filter served to isolate the 18 000–22 500 cm^{-1} spectral region. A total of 50 scans were coadded in about 30 min of observation at an instrumental resolution of 0.1 cm^{-1}. Higher resolution spectra were not recorded because of the large Doppler broadening of the BeH lines. The isolated BeH lines were not always symmetric because of problems with the phase correction.

The spectra were recorded in air so the line positions were first corrected to vacuum wave numbers using the refractive index of air. The wave number scale was then calibrated in the cooler spectrum using Ne lines[23] and this calibration was transferred to the hotter spectrum using strong BeH lines. The estimated absolute accuracy of the wave number scale is ± 0.003 cm^{-1}. The line positions were measured by fitting Voigt line shape functions to the experimental lines in a nonlinear, least-squares procedure using the program SPECTRA. The precision of our measurements is estimated to be about ± 0.01 cm^{-1} for unblended lines.

The experimental setup used to record the $A\ ^2\Pi-X\ ^2\Sigma^+$ $\Delta v=-1$ sequence was previously described in detail by Colin *et al.*[20] in their study of the $C\ ^2\Sigma^+-X\ ^2\Sigma^+$ system and only a brief description will be given here. A conventional arc source with Be electrodes was used to excite the spectrum. The dc arc was operated at 190 V and 9 A, with a 1:5 mixture of H_2 and Ar at a total pressure of a few Torr. The emission spectra were photographed in the second order of a 2 m Czerny–Turner grating spectrograph using Kodak I-F plates and 50 μm slits. The emission spectrum of an iron hollow cathode was used for wavelength calibration. The absolute error in the line positions is estimated to be 0.2 cm^{-1} and the uncertainty in the relative line positions is 0.1 cm^{-1} for strong unblended lines.[20]

III. ANALYSIS

A. Description of the observed bands

An overview of the Fourier transform (FT) emission spectrum of the $A\ ^2\Pi-X\ ^2\Sigma^+$ $\Delta v=0$ sequence of BeH is presented in Fig. 1. The 0–0 to 6–6 bands could be identified in our new spectra. The detection of the 6–6 band is new and the Q lines of the 4–4 and 5–5 bands were also seen for the first time. For the 0–0 to 5–5 bands, the number of assigned lines was extended to both higher and lower N values compared to the previous analyses.[16,20] Some weak and irregular structure was seen near 20 008 cm^{-1} that is probably the 7–7 Q head but no rotational assignments could be made.

All the observed bands have six branches, P_1, P_2, Q_1, Q_2, R_1 and R_2, with the doublet fine structure splitting (F_1 and F_2) resolved at low N values (up to $N\approx 12$ in the case of the cooler spectrum) as appropriate for a Hund's case (b) $^2\Pi-^2\Sigma^+$ transition. As noted first by Watson in 1928, the P, Q, and R branches are very peculiar because a head forms at high N in all three branches. BeH is, therefore, cited in Herzberg[24] as an example of molecule that has ''extra''

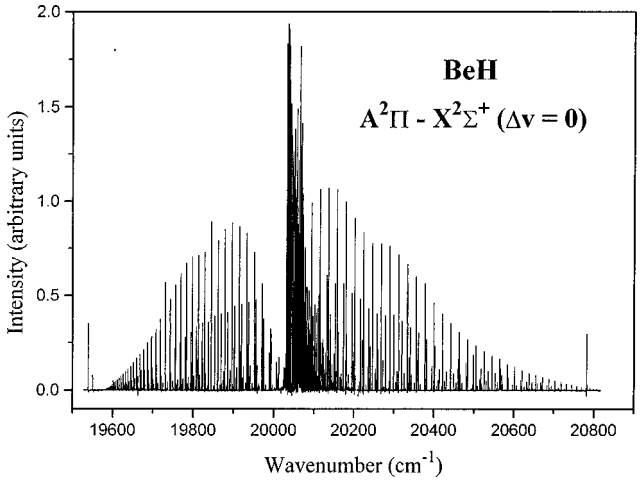

FIG. 1. An overview of the $A\ ^2\Pi - X\ ^2\Sigma^+$ emission spectrum of BeH recorded with a Fourier transform spectrometer.

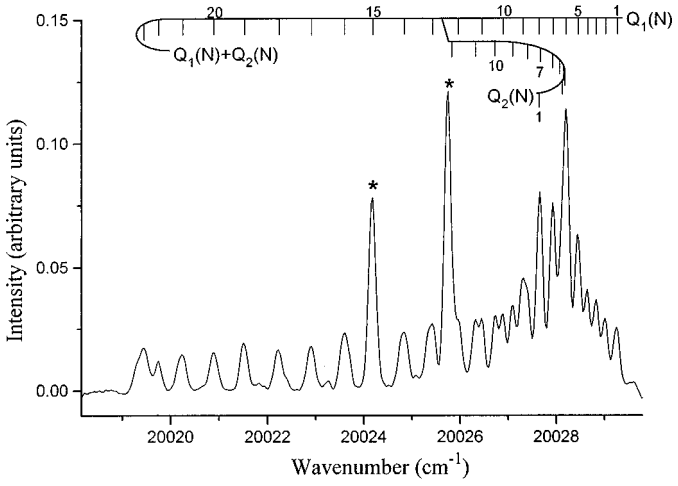

FIG. 2. The 6–6 Q branch of the $A\ ^2\Pi - X\ ^2\Sigma^+$ transition of BeH showing unusual rotational structure. The two lines marked with asterisks are from other bands.

heads. In our hollow cathode spectra, R heads were observed for the 0–0 and 1–1 bands, and ''extra'' Q heads found for the 0–0, 1–1, 2–2 and 3–3 bands (the 4–4, 5–5, and 6–6 Q branches exhibit particularly odd features that will be discussed below). The $A\ ^2\Pi - X\ ^2\Sigma^+$ $\Delta v = 0$ sequence also presents a ''vibrational head'' or ''head-of-heads'' for the Q branches. The origins of the vibrational bands go initially to higher wave numbers with $T_{00} = 20\,030.963\ cm^{-1}$, $T_{11} = 20\,051.310\ cm^{-1}$, $T_{22} = 20\,063.172\ cm^{-1}$, and $T_{33} = 20\,066.248\ cm^{-1}$ and then they turn back to lower wave numbers with $T_{44} = 20\,060.687\ cm^{-1}$, $T_{55} = 20\,047.327\ cm^{-1}$, and $T_{66} = 20\,028.759\ cm^{-1}$. The origins of the 2–2, 3–3, and 4–4 bands are separated only by a few wave numbers so that extensive overlapping of lines occurs. In particular, the 4–4 Q branch is overlapped almost completely by the stronger 2–2 and 3–3 Q branches, and we were able to observe only some ten 4–4 Q lines at low N values.

The 5–5 and 6–6 Q branches also present some interesting aspects caused by the slightly different vibrational dependence of the B_v values in the A and X states. The $B' - B''$ difference is initially positive for the 0–0 band, decreases to zero for the 5–5 band, and becomes slightly negative for the 6–6 band. This fact results in a sharp Q head at 20 047.5 cm^{-1} for the 5–5 band, with the first ten Q lines unresolved. The observation of Q lines and of the first P and R lines in the 4–4 and 5–5 bands allowed us to determine reliable band origins of 20 060.687 cm^{-1} (4–4) and 20 047.327 cm^{-1} (5–5) instead of the previous estimates of 20 062.56 cm^{-1} (4–4) and 20 052.05 cm^{-1} (5–5) based only on P and R lines.[20]

The 6–6 Q branch displayed in Fig. 2 presents a very interesting appearance. The ΔB difference is so small than the two spin components behave differently, with the Q_1 lines starting at $Q_1(N=1) = 20\,029.258\ cm^{-1}$ and going to decreasing wave numbers with increasing N. In contrast, the Q_2 lines start at $Q_2(N=1) = 20\,027.657\ cm^{-1}$, go to higher wave numbers to form a head at 20 028.22 cm^{-1} ($N=3$), and then turn back to lower wave numbers. The two Q branches (unresolved at high N values) then form an ''extra'' head at 20 019.3 cm^{-1} ($N=24$) and return to higher wave numbers as N increases further.

The $A\ ^2\Pi$ state is strongly perturbed by the $C\ ^2\Sigma^+$ as noted by Colin *et al.* in their analysis of the $C\ ^2\Sigma^+ - X\ ^2\Sigma^+$ system.[20] Indeed these perturbations were used to connect the $C\ ^2\Sigma^+$ state and the high vibrational levels of the ground state with the $v''=0$ level of the $X\ ^2\Sigma^+$ state. Colin *et al.* found that the $v=0$, 1, and 2 vibrational levels of the $C\ ^2\Sigma^+$ state were interacting with the $v=4$, 5, 6, and 7 vibrational levels of the $A\ ^2\Pi$ state. In our $A\ ^2\Pi - X\ ^2\Sigma^+$ spectrum, we have observed strongly perturbed P and R lines in the 2–2 to 6–6 bands, while for the 0–0 and 1–1 bands only a few perturbed P and R lines were assigned in the region of the heads. No local perturbations were found in any of the Q branches. For example, one can see that the 6–6 Q branch (displayed in Fig. 2) exhibits no local perturbations up to $N' = 24$, although the P and R lines are already strongly perturbed at $N' = 11$. This fact may be explained by the different interaction of the four ($F_1 e/f$ and $F_2 e/f$) energy levels of a given N of the $A\ ^2\Pi$ state with the two ($F_1 e$ and $F_2 f$) levels of the $C\ ^2\Sigma^+$ state.

The selection rules for perturbations are $\Delta J = 0$, $e-e$, and $f-f$ so that only the e level of the F_1 spin component and the f level of the F_2 component of the $A\ ^2\Pi$ state are perturbed for a $\Delta N = 0$ interaction with the $C\ ^2\Sigma^+$ state. In this case the $Q_2 e-f$ and $Q_1 f-e$ branches will not be perturbed. In principle, $\Delta N = \pm 1$ interactions are possible and they would lead to perturbed Q branches. Experimentally no such perturbed Q branches were detected because the $A\ ^2\Pi$ state belongs to Hund's case (b). N is therefore a good quantum number for both rotations and perturbations so that the $\Delta N = \pm 1$ interactions become very weak.

In order to derive the vibrational intervals, the analysis of a previously recorded[20] arc emission spectrum of the $A\ ^2\Pi - X\ ^2\Sigma^+$ $\Delta v = -1$ sequence was carried out. The 0–1 to 6–7 bands were identified in the 17 800–19 000 cm^{-1} spectral region. Because of the positive $B' - B''$ difference, which is greater than in the $\Delta v = 0$ sequence, the $\Delta v = -1$ bands form ''classical'' P heads. These heads are clearly

TABLE I. Effective constants (in cm^{-1}) for the vibrational levels of the $X\ ^2\Sigma^+$ ground state of BeH (all uncertainties are 1σ).[a]

v	T_v	B_v	$D_v\times10^3$	$H_v\times10^7$	$L_v\times10^{11}$
0	0	10.164 888 0(739)	1.022 969(162)	0.959 35(159)	−0.982 01(704)
1	1 986.4442(103)	9.855 433 5(630)	1.014 180(125)	0.941 908(948)	−1.074 58(237)
2	3 896.8785(185)	9.541 727 1(869)	1.010 671(228)	0.937 35(233)	−1.358 87(782)
3	5 729.2861(312)	9.220 768(100)	1.010 356(320)	0.903 43(403)	−1.765 0(163)
4	7 480.4528(438)	8.886 639(123)	1.017 254(500)	0.827 62(785)	−2.388 4(397)
5	9 145.2834(730)	8.533 209(248)	1.034 38(154)	0.628 5(349)	−2.993(251)
6	10 716.2804(878)	8.152 609(264)	1.074 28(213)	0.327 8(593)	−4.425(524)
7	12 182.323(117)	7.729 457(898)	1.213 79(463)	1.756 3(875)	−27.60(538)
8	13 525.889(123)	7.230 85(128)	1.462 02(863)	4.276(215)	−83.93(177)
9	14 717.860(124)	6.592 13(182)	1.913 4(193)	11.600(782)	−333.0(105)
10	15 709.040(137)	5.698 37(219)	2.758 5(148)	⋯	⋯

[a]An additional parameter [$M=1.810(115)\times10^{-16}\ cm^{-1}$] was determined for the $v=0$ level.

visible in the case of the 0–1 to 3–4 bands but for the 4–5, 5–6, and 6–7 bands they become less prominent as the intensity decreases. The weakness of these lines, along with overlap by stronger Q and R lines of the lower v bands, made the assignment of the 4–5, 5–6, and 6–7 bands very difficult. In addition, the $v=4$, 5, and 6 vibrational levels of the $A\ ^2\Pi$ state begin to be perturbed at low N values (24, 16, and 11 for $v=4$, 5, and 6, respectively) and the corresponding P and R lines are displaced. Fortunately, the Q lines are not perturbed and we were able to follow the Q branches to higher N values than the P and R branches. The presence of these well-behaved Q branches in the $\Delta v=-1$ sequence added some new information to our data set because the high v bands of the $\Delta v=0$ Fourier transform spectroscopy(FTS) measurements had only partly resolved Q branches.

B. Theoretical model and least-squares treatment

We used the usual effective $\hat{\mathbf{N}}^2$ Hamiltonian for $^2\Sigma$ and $^2\Pi$ states[25] to reduce the experimental data to molecular constants. Explicit matrix elements for $^2\Sigma$ and $^2\Pi$ states are provided in Refs. 26 and 27. Because of the extensive amount of high quality data, we needed to use higher-order constants such as M in the $X\ ^2\Sigma^+\ v=0$ level or Λ-doubling parameters up to q_L in some of the vibrational levels of the $A\ ^2\Pi$ state. The matrix elements corresponding to these parameters were calculated by matrix multiplication [e.g., $\mathbf{q}_H=-(\mathbf{Dq}+\mathbf{qD})/2$].

The experimental lines and the ground state combination differences (see below) were fitted using a nonlinear, least-squares procedure with each datum weighted with the square of the reciprocal of the estimated uncertainty. The unblended FTS lines were assigned a weighting factor of 0.01 cm^{-1}, while the $\Delta v=-1$ data were weighted at 0.05 cm^{-1} for the strongest lines and 0.1 cm^{-1} for the weaker ones. However, the measurements of the blended lines were very imprecise in the arc emission spectrum and they were heavily deweighted in the fits.

The main goal of this initial work is a complete characterization of the $X\ ^2\Sigma^+$ ground state, so the perturbed lines in the $\Delta v=0$ sequence were heavily deweighted but the corresponding ground state combination differences were included in the fits. The inclusion of these combination differences greatly improved our determination of the ground state constants and helped to uncouple the two electronic states. They also served as a check for our rotational assignments. We intend to carry out a thorough deperturbation of the $A\ ^2\Pi$ and the $C\ ^2\Sigma^+$ states at a later date.

The main fitting strategy was to work with the $\Delta v=0$ FTS bands first and then use these rotational constants in the $\Delta v=-1$ fits, allowing only the band origins to vary. This strategy was applied for the 0–0 to 4–4 and the 0–1 to 3–4 bands. However, the 4–4, 5–5, and 6–6 bands have peculiar Q branches that were compact and difficult to assign. It turned out that although the Q lines in the $\Delta v=-1$ bands were of lower precision they could be followed to higher N for the 4–5, 5–6, and 6–7 bands than in the 4–4, 5–5 and 6–6 bands. Consequently, we decided to fit all of these bands together and to determine the parameters of the $A\ ^2\Pi$ ($v'=4$, 5, and 6) and $X\ ^2\Sigma^+$ ($v''=5$, 6, and 7) levels simultaneously [the constants for the $X\ ^2\Sigma^+$ ($v''=4$) level were kept fixed at the values determined from the 4–4 fit). These fits gave more reliable values for the Λ-doubling parameters in the $A\ ^2\Pi$ upper state.

The assignment of the 6–7 band linked together the lower vibrational levels ($v''=0-6$) of the ground state with data on the higher vibrational levels, $v''=7-10$, derived from the $C\ ^2\Sigma^+-X\ ^2\Sigma^+$ study.[20] Because the $C\ ^2\Sigma^+\ v=0$, 1, and 2 levels are massively perturbed, only the ground state combination differences were introduced into our fit. In addition to the usual rotational differences, all the possible differences between P lines and R lines with the same N'', N', and v' but different v'' were added to the fit in order to obtain the $X\ ^2\Sigma^+$ vibrational intervals. In this way, the vibrational energy levels for $v''=4-10$ of the ground state were fitted together. The output of this fit, as well as the outputs of the band-by-band fits, has been placed in Physics Auxiliary Publication Service (PAPS).[28] The molecular constants obtained are presented in Tables I and II for the $X\ ^2\Sigma^+$ and $A\ ^2\Pi$ states, respectively.

In the ground $X\ ^2\Sigma^+$ electronic state it was possible to determine the rotational constants B, D, H, and L except for $v=10$ where limited data gave only B and D (Table I). An M constant was also required for $v=0$. A similar set of rotational parameters (Table II) were required for the $A\ ^2\Pi$ state

TABLE II. Molecular constants (in cm^{-1}) for the vibrational levels of the $A\ ^2\Pi$ state of BeH (all uncertainties are 1σ).[a]

Constant	$v=0$	$v=1$	$v=2$	$v=3$	$v=4$	$v=5$	$v=6$
T_{v0}	20 030.962 73(233)	22 037.754 9(124)	23 960.042 1(209)	25 795.566 9(339)	27 541.093 7(493)	29 192.634 1(731)	30 745.046 4(880)
B_v	10.302 101 4(697)	9.970 041 6(643)	9.631 231 9(885)	9.281 843(111)	8.918 924(166)	8.539 357(258)	8.141 314(257)
$D_v\times10^3$	1.042 986(123)	1.039 877(141)	1.041 220(252)	1.045 716(468)	1.050 190(985)	1.069 94(124)	1.163 90(180)
$H_v\times10^7$	0.924 517(852)	0.917 84(123)	0.913 97(291)	0.914 17(853)	0.810 2(286)	0.414 5(138)	0.264 2(142)
$L_v\times10^{11}$	−0.949 73(197)	−1.130 82(376)	−1.419 4(115)	−2.113 5(538)	−3.296(270)	⋯	⋯
A_v	2.154 3(142)	2.132 5(126)	2.185 7(164)	2.223 9(157)	2.171 5(184)	2.248 3(319)	2.194 4(242)
$\gamma_v\times10^3$	−7.778(295)	−5.955(194)	−8.146(252)	−8.760(333)	−8.094(618)	−5.031(727)	−4.461(344)
$\gamma_{Dv}\times10^6$	7.790(504)	3.588(193)	6.504(314)	8.451(669)	6.45(175)	⋯	⋯
$q_v\times10^2$	1.402 65(284)	1.348 99(381)	1.266 34(496)	1.191 28(268)	1.143 5(213)	1.103 1(339)	1.193 6(246)
$q_{Dv}\times10^6$	−6.217 8(800)	−6.656(137)	−6.758(233)	−7.091 6(540)	−12.774(465)	−25.71(176)	−157.96(268)
$q_{Hv}\times10^9$	1.408 7(697)	1.814(158)	2.118(346)	⋯	⋯	⋯	⋯
$q_{Lv}\times10^{13}$	−3.002(190)	−5.810(578)	−1.247(163)	⋯	⋯	⋯	⋯

[a]An additional parameter [$\gamma_H=-2.220(198)\times10^{-9}$ cm^{-1}] was determined for the $v=0$ level.

TABLE III. Dunham constants (in cm^{-1}) for the $X\ ^2\Sigma^+$ ground state of BeH (all uncertainties are 1σ).

	$m=0$	$m=1$	$m=2$	$m=3$	$m=4$	$m=5$
$Y_{0,m}$		10.331 214 7(5042)	$-1.044\ 176\ 0(6760)\times10^{-3}$	$1.024\ 361(3302)\times10^{-7}$	$-9.539\ 09(8802)\times10^{-12}$	$1.6404(1326)\times10^{-16}$
$Y_{1,m}$	2068.863 4(5174)	−0.351 068(1721)	$6.654\ 3(2154)\times10^{-5}$	$-2.174\ 24(8582)\times10^{-8}$	$1.042(1000)\times10^{-13}$	
$Y_{2,m}$	−46.145 5(6352)	$4.833\ 4(1856)\times10^{-2}$	$-5.964\ 6(2101)\times10^{-5}$	$2.023\ 18(7169)\times10^{-8}$	$-9.289\ 4(3947)\times10^{-13}$	
$Y_{3,m}$	4.980 9(3694)	$-2.527\ 35(9045)\times10^{-2}$	$2.657\ 77(8897)\times10^{-5}$	$-7.807\ 2(2579)\times10^{-9}$		
$Y_{4,m}$	−1.612 0(1167)	$6.668\ 9(2266)\times10^{-3}$	$-6.006\ 1(1813)\times10^{-6}$	$1.385\ 47(4124)\times10^{-9}$		
$Y_{5,m}$	0.289 17(2120)	$-9.657\ 1(3021)\times10^{-4}$	$6.434\ 1(1733)\times10^{-7}$	$-9.749\ 9(2338)\times10^{-11}$		
$Y_{6,m}$	$-3.097\ 8(2210)\times10^{-2}$	$7.065\ 8(2031)\times10^{-5}$	$-2.608\ 59(6180)\times10^{-8}$			
$Y_{7,m}$	$1.783\ 9(1228)\times10^{-3}$	$-2.102\ 43(5411)\times10^{-6}$				
$Y_{8,m}$	$-4.445\ 3(2817)\times10^{-5}$					

TABLE IV. Main equilibrium constants (in cm^{-1}) of the $A\ ^2\Pi$ state of BeH[a,b] (all uncertainties are 1σ).

$T_e = 20\,019.7647(146)$	
$\omega_e = 2089.953\,0(421)$	$B_e = 10.466\,305(273)$
$\omega_e x_e = 41.363\,9(303)$	$\alpha_e = 0.327\,746(405)$
$\omega_e y_e = -0.074\,83(766)$	$\gamma_{1e} = -0.001\,237(157)$
$\omega_e z_e = -0.037\,98(617)$	$\gamma_{2e} = -0.000\,519\,3(166)$

[a] $G_v = \omega_e(v+\frac{1}{2}) - \omega_e x_e(v+\frac{1}{2})^2 + \omega_e y_e(v+\frac{1}{2})^3 + \omega_e z_e(v+\frac{1}{2})^4$.
[b] $B_v = B_e - \alpha_e(v+\frac{1}{2}) + \gamma_{1e}(v+\frac{1}{2})^2 + \gamma_{2e}(v+\frac{1}{2})^3$.

along with the Λ-doubling series q, q_D, q_H, and q_L as well as the spin–orbit coupling constant A and the spin–rotation constants γ and γ_D.

The $A\ ^2\Pi$ and $X\ ^2\Sigma^+$ electronic states of BeH both belong to the Hund's case (b) coupling case, and this led to strong correlation between the spin–rotation parameters γ' and γ''. No satellite branches were detected so γ'' could not be directly determined. We have therefore chosen to fix the ground state γ constant to zero and to vary the corresponding constant in the upper state. The Λ-doubling constant p also could not be determined because of the nearly pure case b coupling in the $A\ ^2\Pi$ state.

A second stage in our analysis was to fit all the available data together, including the vibrational levels $v''=0$ to 10 for the $X\ ^2\Sigma^+$ state and $v'=0-6$ for the $A\ ^2\Pi$ state in a global fit to determine Dunham constants[29] in the ground state. In this case, the ground state rovibrational energies were represented by the conventional double Dunham expansion,[29]

$$E_X(v'',N'') = \sum_{l,m} Y''_{l,m}\left(v''+\frac{1}{2}\right)^l [N''(N''+1)]^m, \qquad (1)$$

and the upper $A\ ^2\Pi$ levels were represented by the same $^2\Pi$ matrix discussed above. The values of the $Y''_{l,m}$ parameters obtained are listed in Table III. However, it should be noted that the normalized standard deviation of 1.8 of this fit was somewhat higher than the values of about 1 obtained in the separate fits described above. The equilibrium vibrational and rotational constants were also derived for the $A\ ^2\Pi$ state using the constants listed in Table II and the equilibrium parameters are presented in Table IV.

IV. DISCUSSION

The new Fourier transform spectra of the $A\ ^2\Pi - X\ ^2\Sigma^+$ system greatly improved the spectroscopic constants and also cleared up some spectroscopic mysteries. One puzzling feature in the spectra was the appearance of two groups of unassigned lines to lower wave numbers of the strong 0–0 Q branch. They are the tiny features on the left-hand side of the 0–0 Q branch in Fig. 1 (see also Fig. 2). These lines look like peculiar Q branches and they were noted even in early arc spectra of Watson and Parker.[12] In fact the presence of many additional P and R lines in the $A\ ^2\Pi - X\ ^2\Sigma^+$ transition led Watson and Parker to the erroneous conclusion that they had found the ^{8}BeH isotopomer. They understood that the $A-X$ system had a head-of-heads at the 4–4 band and they assigned the two extra Q branches to the 8–8 and 9–9 bands. The head-of-heads in fact forms at the 3–3 band and these extra two Q heads turn out to belong to the 6–6 and 7–7 bands, but Watson and Parker were clearly on the right track.

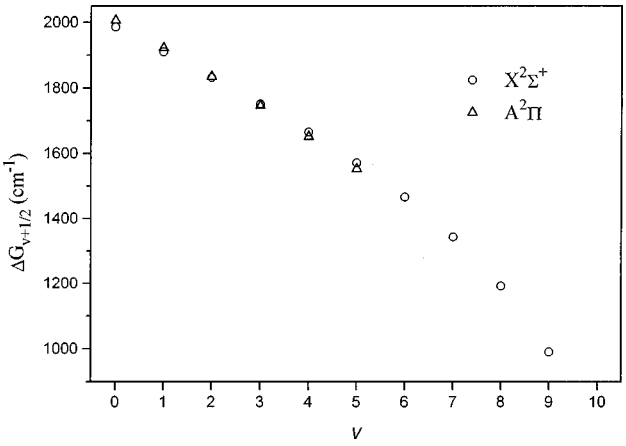

FIG. 3. A plot of $\Delta G_{v+1/2}$ as a function of v for the $A\ ^2\Pi$ and $X\ ^2\Sigma^+$ states of BeH.

The various parameters (Table II) in the excited $A\ ^2\Pi$ state empirically account for the observed spectroscopic features. The long series of Λ-doubling parameters (q's) are necessary because the Q branches connect to excited state rotational levels of opposite parity compared to the P and R branches. This leads to a combination defect between the Q branches and the P and R branches that would normally be small. In this case the $C\ ^2\Sigma^+$ state is nearby and the strong local interactions require as many q parameters as there are terms in the B series of parameters. The q series of parameters thus lets the e and f parity levels have slightly different effective rotational constants.

The spin splitting is resolved only at low N values and disappears as the spin uncoupling becomes complete. This splitting is represented in the $A\ ^2\Pi$ state by the spin–orbit coupling constant A and the two spin–rotation constants γ and γ_D. Since A_D and γ are completely correlated[30] for a $^2\Pi$ state, we have chosen to determine γ because the $A\ ^2\Pi$ state is close to Hund's case (b). The effect of the constants γ and

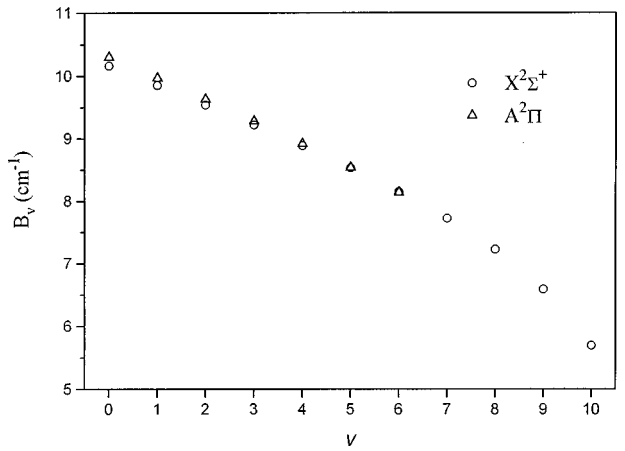

FIG. 4. A plot of B_v as a function of v for the $A\ ^2\Pi$ and $X\ ^2\Sigma^+$ states of BeH.

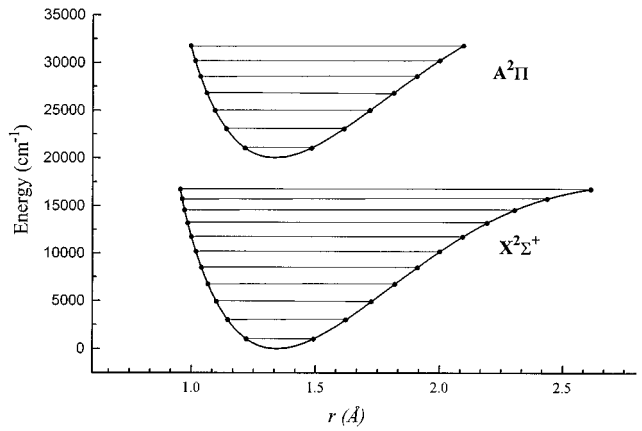

FIG. 5. The RKR potential energy curves for the $A\ ^2\Pi$ and $X\ ^2\Sigma^+$ states of BeH.

γ_D is to allow the F_1 and F_2 spin components to have slightly different effective B values while the A constant, as usual, is the rotationless spin–orbit splitting.

Since we have arbitrarily set the spin–rotation constant γ'' to zero in the ground state, the exited state constant γ' is, in fact, the difference $\gamma'-\gamma''$. In this respect the $A\ ^2\Pi-X\ ^2\Sigma^+$ transition is like a $^2\Sigma-^2\Sigma$ transition. It is possible to estimate a value of $\gamma''=2(2)\times10^{-3}$ cm^{-1} for the ground state using Curl's relationship,[31,32] $\gamma=2B\Delta g$, and the small anisotropy of the g tensor of matrix-isolated BeH.[33] A crude estimate based on a pure precession relationship[34] between the ground state and the $A\ ^2\Pi$ state gives a similar value of $\gamma''=4\times10^{-3}$ cm^{-1}. Note that pure precession also implies that the experimentally undetermined Λ-doubling parameter p $(=\gamma'')$ has the same value of 4×10^{-3} cm^{-1} in the $A\ ^2\Pi$ state.

The $A\ ^2\Pi$ and $X\ ^2\Sigma^+$ states have remarkably similar vibrational and rotational constants as is illustrated graphically in Figs. 3 and 4. In Fig. 3, $\Delta G'_{1/2}>\Delta G''_{1/2}$ and the diagonal bands go to higher wave numbers as v increases but a head-of-head forms when the difference in $\Delta G_{v+1/2}$ values becomes negative after the 3–3 band. In the B_v plot (Fig. 4), the excited state B_v values are initially greater than in the ground state for the diagonal bands and the Q branches go to higher wave numbers as N increases (Fig. 1). At the 5–5 band, however, the ground and excited state B_v values become identical (Fig. 4) and a linelike Q branch results, although because of centrifugal distortion some lines are resolved at higher N values in the hotter spectrum. The peculiar 6–6 Q branch (Fig. 2) has already been discussed.

The Dunham constants of Table III are a poor representation of the energy levels of BeH. This is a well-known fact for hydrides[8] and is a particular problem for H_2. The traditional constants form a badly convergent series with strong correlation between the parameters. It is, therefore, necessary to carry many extra significant figures in Table III and many of the terms (even ω_e) in the expansion have lost much of their physical meaning. Nevertheless, the Y's of Table III do reproduce the experimental data in an empirical manner. In future work, we plan to explore the fitting of the BeH and BeD data using alternate energy level expressions[35] as well as the direct fitting to a potential energy curve that includes Born–Opppenheimer breakdown terms.[36]

The $B_v(Y_{i1})$ and $G_v(Y_{i0})$ functions (Table III) were used to calculate the Rydberg–Klein–Rees (RKR) potential energy curve plotted for the ground state shown in Fig. 5. As can be seen in Fig. 5, $v=10$ is the last bound vibrational level although it is difficult to rule out[37] a $v=11$ level bound by a few cm^{-1}. Interestingly, the outer turning points of $v=9$ and 10 are not in the long-range region so a LeRoy–Bernstein analysis[38] of the G_v data (Fig. 3) is not appropriate.

The $A\ ^2\Pi$ excited state rotational constants and band origins (Table II) were fitted with the traditional expressions (Table IV) to obtain equilibrium constants. The equilibrium bond length for the $A\ ^2\Pi$ state was calculated to be 1.332 99(2) Å compared to 1.341 68(3) Å for the ground state, calculated from Y_{01} (Table III). The equilibrium constants of Table IV were used to calculate the $A\ ^2\Pi$ state RKR potential curve also displayed in Fig. 5. The RKR turning points are available from the authors upon request.

The RKR potential energy curves were used to calculate the Franck–Condon factors (Table V). A glance at Table V explains why we were not able to see the $\Delta v=-1$ sequence in spite of the excellent signal-to-noise ratio (Fig. 1) obtained for $\Delta v=0$ bands. For the $\Delta v=-1$ bands, the largest Franck–Condon factor is 0.0042 for the 2–3 band so that we were forced to use the older arc measurements to see the bands. Note that since we only used the $\Delta v=-1$ sequence, all of the systematic errors in the calibration of the photographic plates propagate upwards so that the $v=10$ level could be in error by as much as 2 cm^{-1}.

V. CONCLUSION

We have measured the 0–0 to 6–6 bands of the $A\ ^2\Pi-X\ ^2\Sigma^+$ transition of BeH with a Fourier transform spectrometer. These bands show many unusual features such

TABLE V. Franck–Condon factors for the $A\ ^2\Pi-X\ ^2\Sigma^+$ transition of BeH.

v'	v''	0	1	2	3	4	5	6	7	8	9	10
0		0.998	2.07$E-3$	5.00$E-5$	1.11$E-6$	4.42$E-8$	5.86$E-9$	7.26$E-6$	8.56$E-6$	4.24$E-9$	1.17$E-6$	1.72$E-7$
1		2.09$E-3$	0.994	3.59$E-3$	1.69$E-4$	3.57$E-6$	4.36$E-5$	7.49$E-7$	8.23$E-6$	1.27$E-5$	1.11$E-5$	6.57$E-6$
2		2.05$E-5$	3.72$E-3$	0.992	4.18$E-3$	3.47$E-4$	1.05$E-5$	1.04$E-7$	9.65$E-6$	2.11$E-5$	2.24$E-5$	1.86$E-5$
3		2.73$E-5$	8.00$E-5$	4.41$E-3$	0.991	3.96$E-3$	5.74$E-4$	2.56$E-5$	4.04$E-4$	2.79$E-5$	6.18$E-5$	5.32$E-5$
4		5.63$E-7$	2.86$E-5$	2.10$E-4$	4.27$E-3$	0.992	3.09$E-3$	8.24$E-4$	5.41$E-5$	1.66$E-6$	3.80$E-5$	1.33$E-4$
5		1.55$E-6$	5.10$E-5$	6.44$E-04$	4.23$E-4$	3.42$E-3$	0.993	1.85$E-3$	1.07$E-3$	9.70$E-5$	7.38$E-6$	4.14$E-5$
6		8.07$E-6$	9.89$E-6$	2.35$E-04$	5.10$E-6$	7.06$E-4$	2.10$E-3$	0.995	5.44$E-4$	1.38$E-3$	1.35$E-4$	1.97$E-5$

as a head-of-heads and peculiar Q branches as the result of the near identity of the spectroscopic constants in the two states. By assigning the 0–1 to 6–7 bands in the $\Delta v=-1$ sequence in an archival arc emission spectrum, we were able to link together all of the new FTS data as well as connect with the $C\ ^2\Sigma^+-X\ ^2\Sigma^+$ bands which cover $v''=7-10$. BeH thus joins the small set of chemically bound molecules for which all of the ground state vibrational levels have been derived from high-resolution data.

ACKNOWLEDGMENTS

This work was supported by the Fonds National de la Recherche Scientifique (Belgium) and the Natural Sciences and Engineering Research Council of Canada. C.F. thanks the Université des Sciences et Technologies de Lille (France) for a BQR grant. We thank R. LeRoy, M. Carleer, and R. Mitzner for their help and for discussions.

[1] W. Meyer and P. Rosmus, J. Chem. Phys. **63**, 2356 (1975).
[2] D. L. Cooper, J. Chem. Phys. **80**, 1961 (1984).
[3] M. Larsson, Phys. Scr. **32**, 97 (1985).
[4] C. Henriet and G. Verhaegen, Phys. Scr. **33**, 299 (1986).
[5] I. D. Petsalakis, G. Theodorakopoulos, and C. A. Nicolaides, J. Chem. Phys. **97**, 7623 (1992).
[6] I. D. Petsalakis, R. J. Buenker, G. Hirsch, and G. Theodorakopoulos, J. Phys. B **30**, 4935 (1997).
[7] F. B. C. Machado, O. Roberto-Neto, and F. R. Ornellas, Chem. Phys. Lett. **284**, 293 (1998).
[8] J. M. L. Martin, Chem. Phys. Lett. **283**, 283 (1998).
[9] B. Fernandez and P. Jorgensen, Chem. Phys. Lett. **232**, 463 (1995).
[10] W. W. Watson, Phys. Rev. **32**, 600 (1928).
[11] E. Olsson, Z. Phys. **73**, 732 (1932).
[12] W. W. Watson and A. E. Parker, Phys. Rev. **37**, 167 (1931).
[13] W. W. Watson and R. F. Humphreys, Phys. Rev. **52**, 318 (1937).
[14] P. G. Koontz, Phys. Rev. **48**, 707 (1935).
[15] G. Duxbury, M. F. Stamp, and H. P. Summers, Plasma Phys. Controlled Fusion **40**, 361 (1998).
[16] R. Horne and R. Colin, Bull. Soc. Chim. Belges **81**, 93 (1972).
[17] R. Colin, D. De Greef, P. Goethals, and G. Verhaegen, Chem. Phys. Lett. **25**, 70 (1974).
[18] D. De Greef and R. Colin, J. Mol. Spectrosc. **53**, 455 (1974).
[19] R. Colin and D. De Greef, Can. J. Phys. **53**, 2142 (1975).
[20] R. Colin, C. Drèze, and M. Steinhauer, Can. J. Phys. **61**, 641 (1983).
[21] C. Clerbaux and R. Colin, Mol. Phys. **72**, 471 (1991).
[22] T. J. Tague, Jr. and L. Andrews, J. Am. Chem. Soc. **115**, 12111 (1993).
[23] B. A. Palmer and R. Engleman, Jr., *Atlas of the Thorium Spectrum* (Los Alamos National Laboratory, Los Alamos, NM, 1983).
[24] G. Herzberg, *Spectra of Diatomic Molecules*, 2nd ed. (Van Nostrand, New York, 1950), pp. 174–175.
[25] J. M. Brown, E. A. Colbourne, J. K. G. Watson, and F. D. Wayne, J. Mol. Spectrosc. **74**, 425 (1979).
[26] M. Douay, S. A. Rogers, and P. F. Bernath, Mol. Phys. **64**, 425 (1988).
[27] C. Amiot, J.-P. Maillard, and J. Chauville, J. Mol. Spectrosc. **87**, 196 (1981).
[28] See AIP Document # PAPS: JCPSA 6-109-002838 for 52 pages of tables. Order by PAPS number and journal reference from American Institute of Physics, Physics, Physics Auxillary Publication Service, Carolyn Gehlbach, 500 Sunnyside Boulevard, Woodbury, NY 11797-2999. Fax: 516-576-2223, e-mail: paps@aip.org. The price is $1.50 for each microfiche (98 pages) or $5.00 for photocopies of up to 30 pages, and $0.15 for each additional page over 30 pages. Airmail additional. Make checks payable to the American Institute of Physics.
[29] J. L. Dunham, Phys. Rev. **41**, 721 (1932).
[30] J. M. Brown and J. K. G. Watson, J. Mol. Spectrosc. **65**, 65 (1977).
[31] R. F. Curl, Jr., J. Chem. Phys. **37**, 779 (1962).
[32] W. Weltner, Jr., *Magnetic Atoms and Molecules* (Dover, New York, 1990).
[33] L. B. Knight, Jr., J. M. Brom, Jr., and W. Weltner, Jr., J. Chem. Phys. **56**, 1152 (1972).
[34] J. H. Van Vleck, Phys. Rev. **33**, 467 (1929).
[35] D. T. Appadoo *et al.*, J. Chem. Phys. **104**, 903 (1996).
[36] M. Dulick, K.-Q. Zhang, B. Guo, and P. F. Bernath, J. Mol. Spectrosc. **188**, 14 (1998).
[37] Preliminary calculations by R. J. LeRoy indicate that $v=11$ is bound by about 50 cm^{-1}.
[38] R. J. LeRoy and R. B. Bernstein, Chem. Phys. Lett. **5**, 42 (1970).